

## Supplementary Materials for

# **Mechanobiological Modulation of Blood-Brain Barrier Permeability by Laser Stimulation of Endothelial-Targeted Nanoparticles**

Xiaoqing Li,<sup>a§</sup> Qi Cai,<sup>b§</sup> Blake A. Wilson,<sup>b</sup> Hanwen Fan,<sup>b</sup> Harsh Dave,<sup>a</sup> Monica Giannotta,<sup>c\*</sup> Robert Bachoo,<sup>d,e,f\*</sup> and Zhenpeng Qin<sup>a,b,g,h\*</sup>

<sup>a</sup>Department of Bioengineering, the University of Texas at Dallas, Richardson, TX 75080, USA

<sup>b</sup>Department of Mechanical Engineering, the University of Texas at Dallas, Richardson, TX 75080 USA

<sup>c</sup>Institute of Molecular Oncology Foundation (IFOM), 20139 Milan, Italy

<sup>d</sup>Department of Internal Medicine, the University of Texas Southwestern Medical Center, Dallas, TX75390, USA

<sup>e</sup>Harold C. Simmons Comprehensive Cancer Center, the University of Texas Southwestern Medical Center, Dallas, TX75390, USA.

<sup>f</sup>Department of Neurology, the University of Texas Southwestern Medical Center, Dallas, TX75390, USA

<sup>g</sup>Center for Advanced Pain Studies, the University of Texas at Dallas, Richardson, TX 75080, USA

<sup>h</sup>Department of Surgery, University of Texas Southwestern Medical Center, Dallas, TX75390, USA

This PDF includes:

Figure S1-12

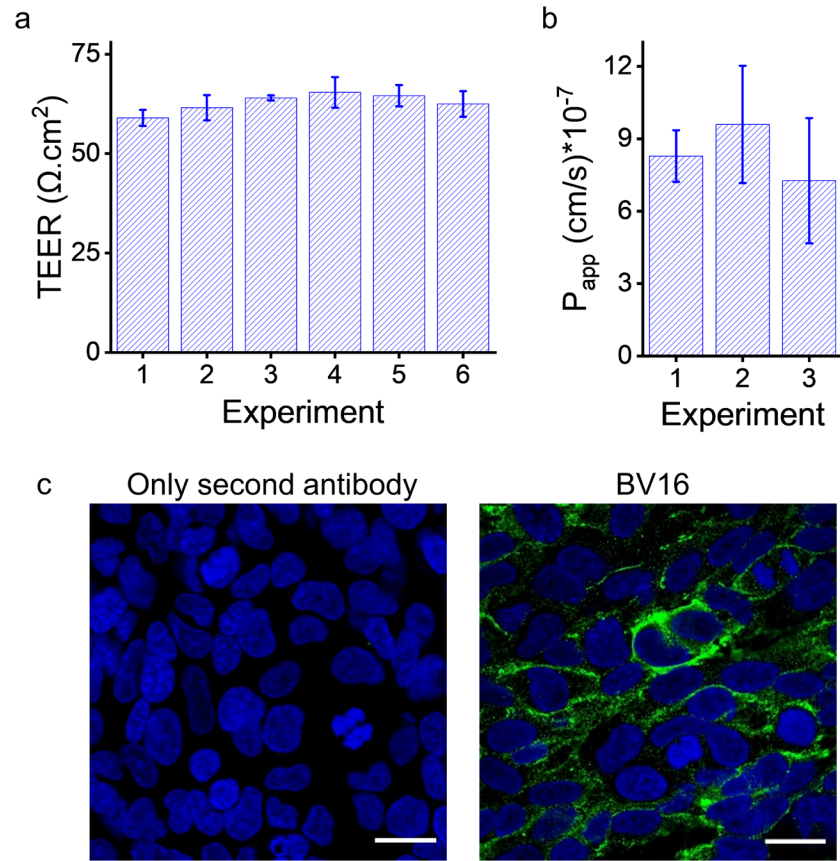


**Figure S1. Characterization of *in vitro* BBB model using hCMEC/D3 monolayers. (a)** Transendothelial electrical resistance (TEER) of D3 monolayers. 3 replicates in each experiment. **(b)** Permeability to FITC-dextran (40 kDa) of D3 monolayers. 3 replicates in each experiment. **(c)** Formation of tight junctions detected by ICC staining. Green: JAM-A detected by BV16. Blue: nuclei. Data expressed as Mean  $\pm$  SD. Scale bar: 10  $\mu\text{m}$ .

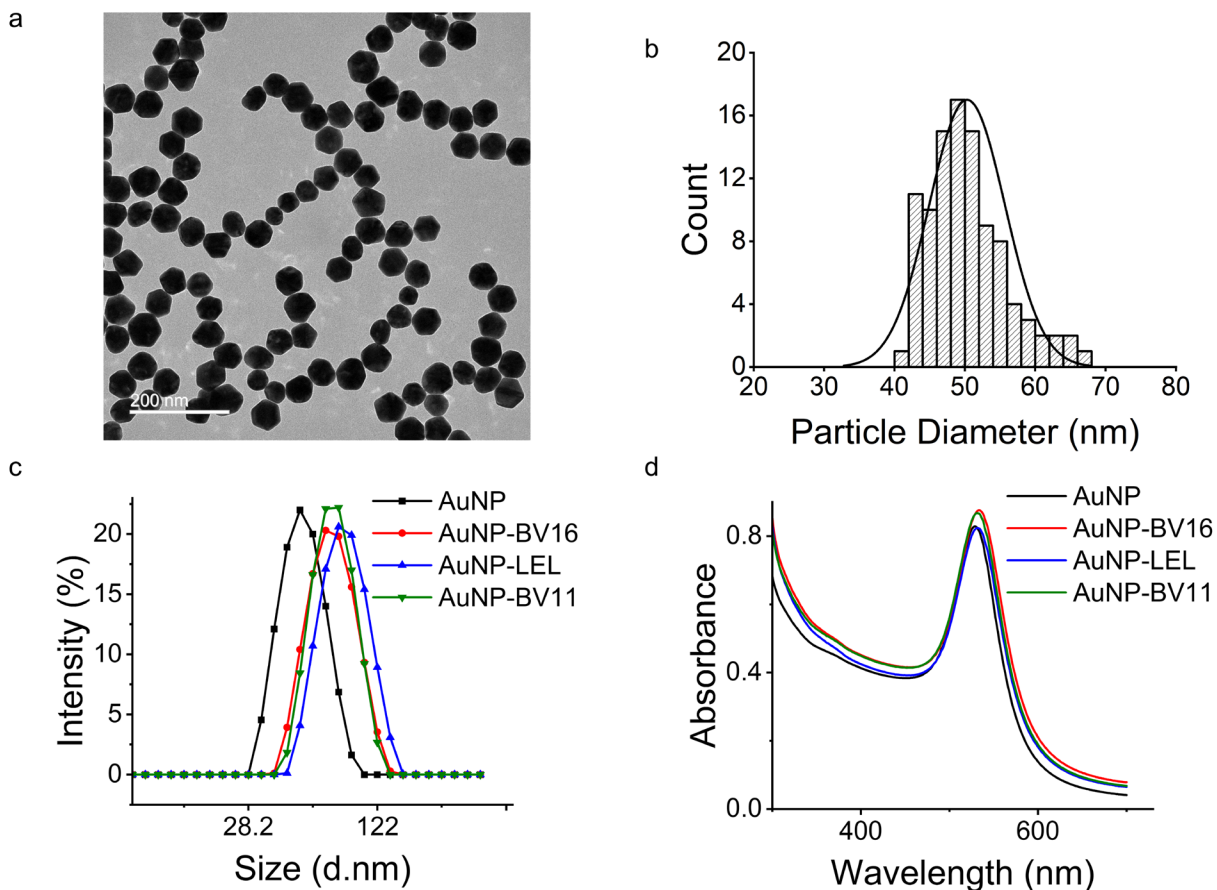


**Figure S2. Characterization of AuNPs modified with different targets.** (a-b) TEM image and size distribution of the AuNPs. The size of the particles was  $50 \pm 5$  nm. 100 particles were counted manually with Image-J. Scale bar: 200 nm. (c) Size distribution by DLS of AuNPs modified with BV16 (mouse anti-human JAM-A antibody), LEL (*Lycopersicon esculentum* lectin for targeting glycoprotein), and BV11 (rat anti-mouse JAM-A antibody). (d) Localized surface plasmon resonance of AuNP, AuNP-BV16, AuNP-LEL and AuNP-BV11 measured by UV-Vis-Vis spectroscopy.

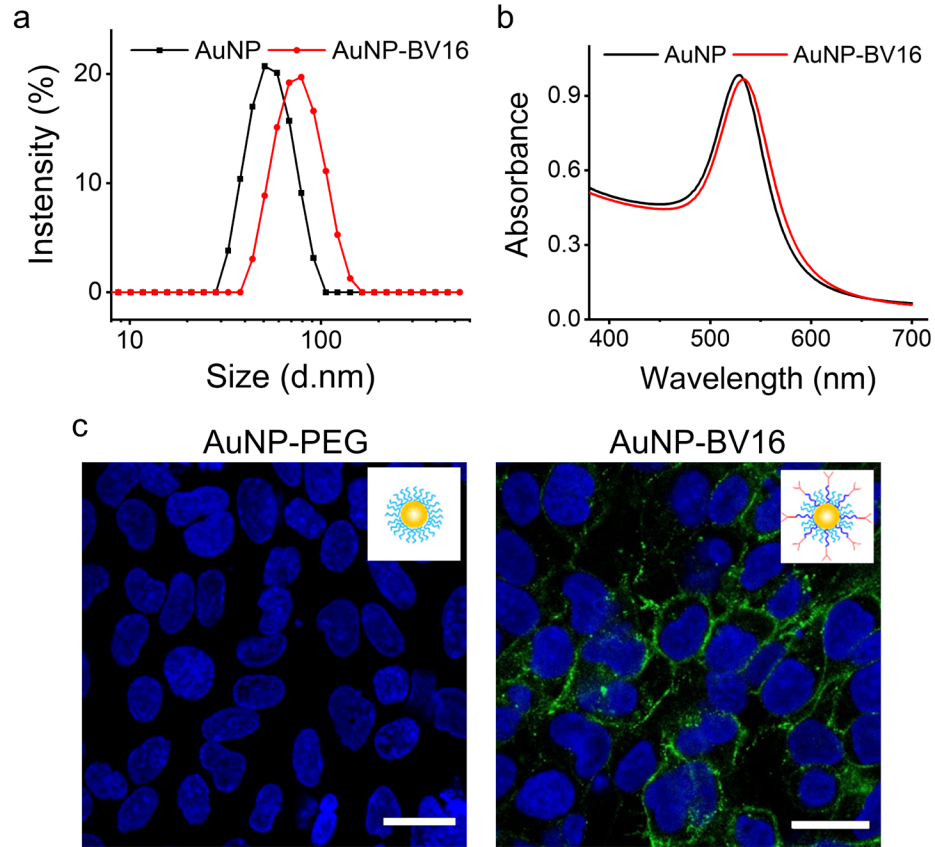


**Figure S3. Characterization and targeting of AuNP-BV16.** (a-b) Characterization of AuNP-BV16 by DLS (a) and UV-vis spectroscopy (b). (c) Tight junction targeted by AuNP-BV16 (0.5 nM) using ICC staining, while non-targeting AuNP (AuNP-PEG) does not show specific targeting. Green: JAM-A stained by AuNP-BV16. Blue: nuclei. Scale bar: 10  $\mu$ m.

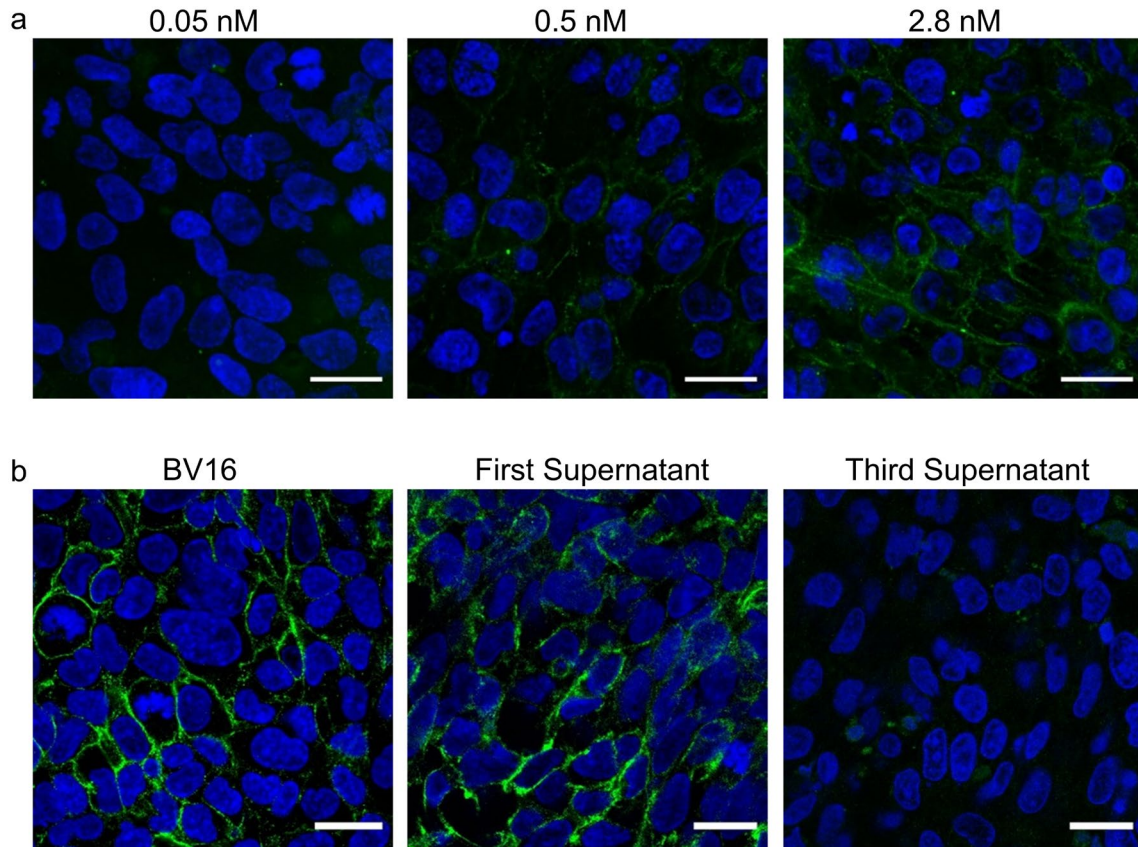


**Figure S4. Optimization of AuNP-BV16 for OptoBBB. (a)** Distribution of TJ-targeting AuNP (AuNP-BV16) on D3 monolayers with various AuNP concentrations. Obvious TJ targeting using 0.5 nM and 2.8 nM AuNP-BV16 was observed, but not 0.05 nM AuNP-BV16. Thus, 0.5 nM AuNP-BV16 was selected for OptoBBB *in vitro*. **(b)** Lack of free antibody in the AuNP-BV16 conjugate. The free BV16 will compete with AuNP-BV16 for JAM-A binding, which affects AuNP-BV16 targeting. The first supernatant and third supernatant were incubated with monolayers, respectively, to confirm if there were free BV16 after washing. The free antibody had been removed after washing 3 times indicated by the right panel image, which doesn't show green signal. BV16: free BV16 antibody as positive control, first supernatant: supernatant from AuNP-BV16 conjugation after washing 1 time. Third supernatant: supernatant from AuNP-BV16 conjugation after washing 3 times. Scale bar: 10  $\mu\text{m}$ .

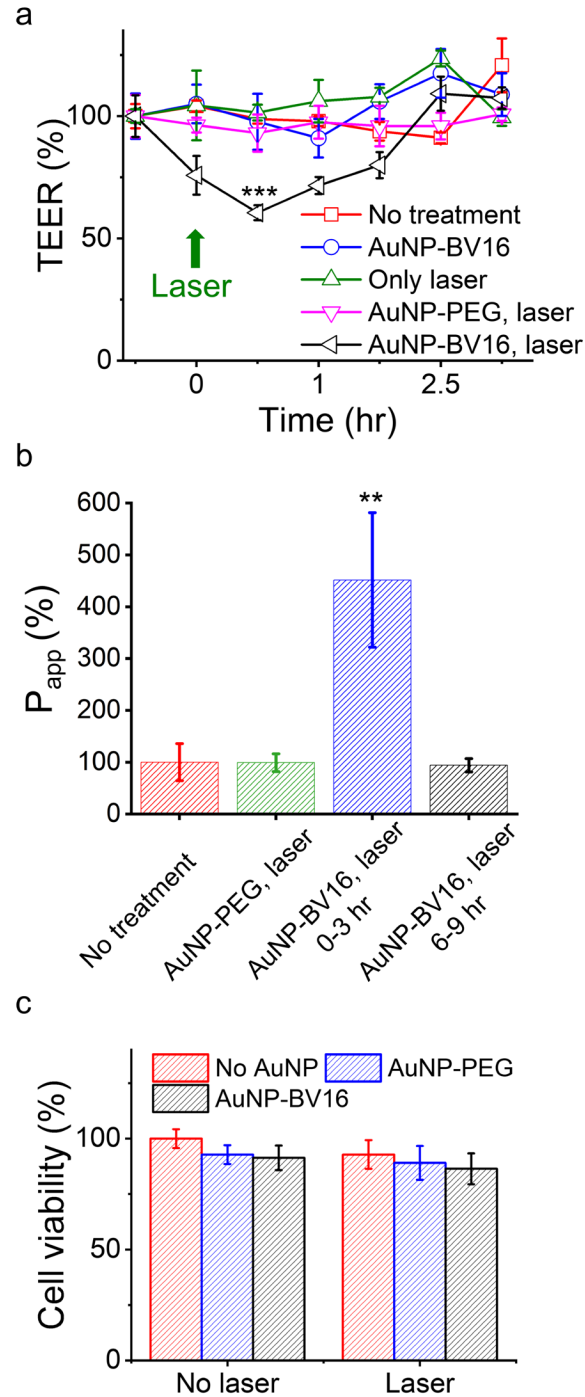


**Figure S5. Reversible BBB opening by laser excitation of AuNP-BV16.** (a) Normalized TEER change over time by laser stimulation. n=3 replicates. (b) Reversible permeability changes after laser stimulation. n=3 replicates. (c) No significant difference in cell viability after laser stimulation. n=6 replicates. Incubation concentration: 0.5 nM, laser: 35mJ/cm<sup>2</sup>, 25 pulses, 5 Hz. Data expressed as Mean ± SD. Unpaired *t*-test was performed individually between No treatment (No laser and No AuNP) and the other groups. \*\*: P<0.01, or \*\*\* P<0.001 was considered a statistically significant difference.

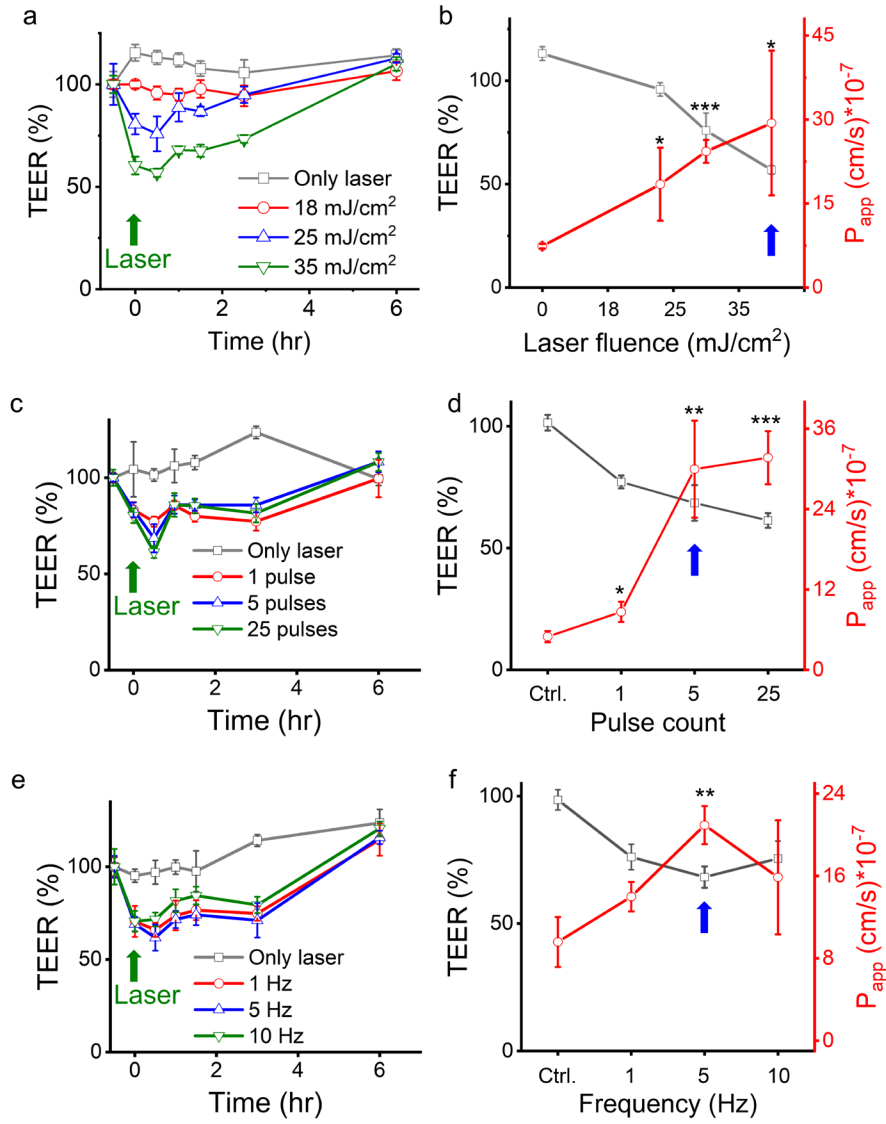


**Figure S6. Effects of laser parameters on OptoBBB. (a-b)** TEER (a) and permeability (b) change after laser stimulation under different laser fluences. 25 pulses, 5 Hz. **(c-d)** TEER (c) and permeability (d) change after laser stimulation under different laser pulse counts. 35  $\text{mJ/cm}^2$ , 5 Hz. **(e-f)** TEER (e) and permeability (f) change after laser stimulation with different frequencies. 35  $\text{mJ/cm}^2$ , 25 pulses. Data expressed as Mean  $\pm$  SD ( $n=3$ ). Unpaired  $t$ -test was performed for permeability individually between Only laser and the other groups. \*\*:  $P < 0.01$  was considered a statistically significant difference. The blue arrow indicates the condition selected for the following experiments.

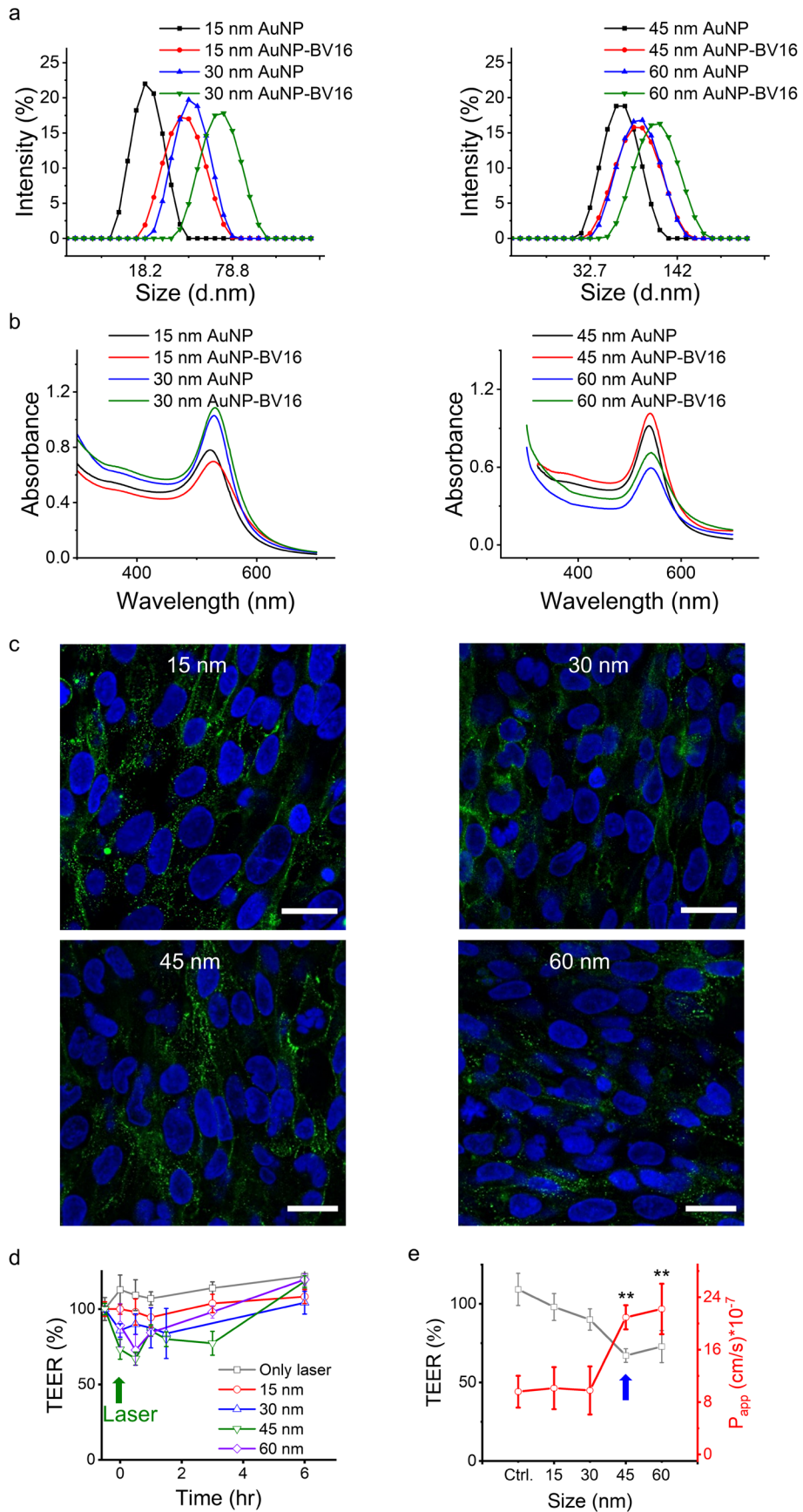




**Figure S7. Effects of AuNP size on the BBB opening. (a-b)** Characterization of AuNP-BV16 with particle sizes of 15, 30, 45, and 60 nm using DLS (a) and UV-vis spectrum (b). **(c)** Distribution of AuNP-BV16 on D3 monolayers with sizes 15, 30, 45, and 60 nm. **(d-e)** TEER (d) and permeability (e) change of D3 monolayers with laser excitation of AuNP with sizes 15, 30, 45, and 60 nm. Data expressed as Mean  $\pm$  SD (n=3). Unpaired *t*-test was performed for permeability individually between Only laser and the other groups. \*\*: P<0.01 was considered a statistically significant difference. The Blue arrow indicates the condition selected for the following experiments. Scale bar: 10  $\mu$ m.

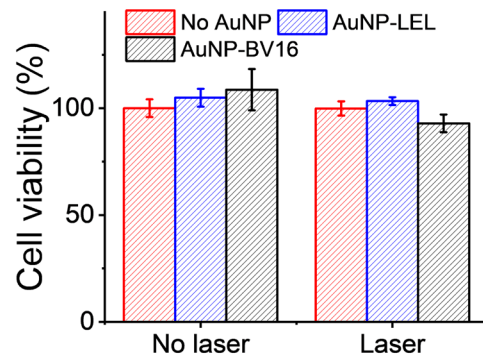


**Figure S8. Cell viability after laser excitation of different targeting AuNPs.** AuNP-LEL: 0.02 nM, AuNP-BV16: 0.5 nM. 35mJ/cm<sup>2</sup>, 5 pulses, 5 Hz. Data expressed as Mean  $\pm$  SD (n=6). Unpaired *t*-test was performed individually between the no treatment (No AuNP w/ No laser) group and the other groups. No significant difference was observed.

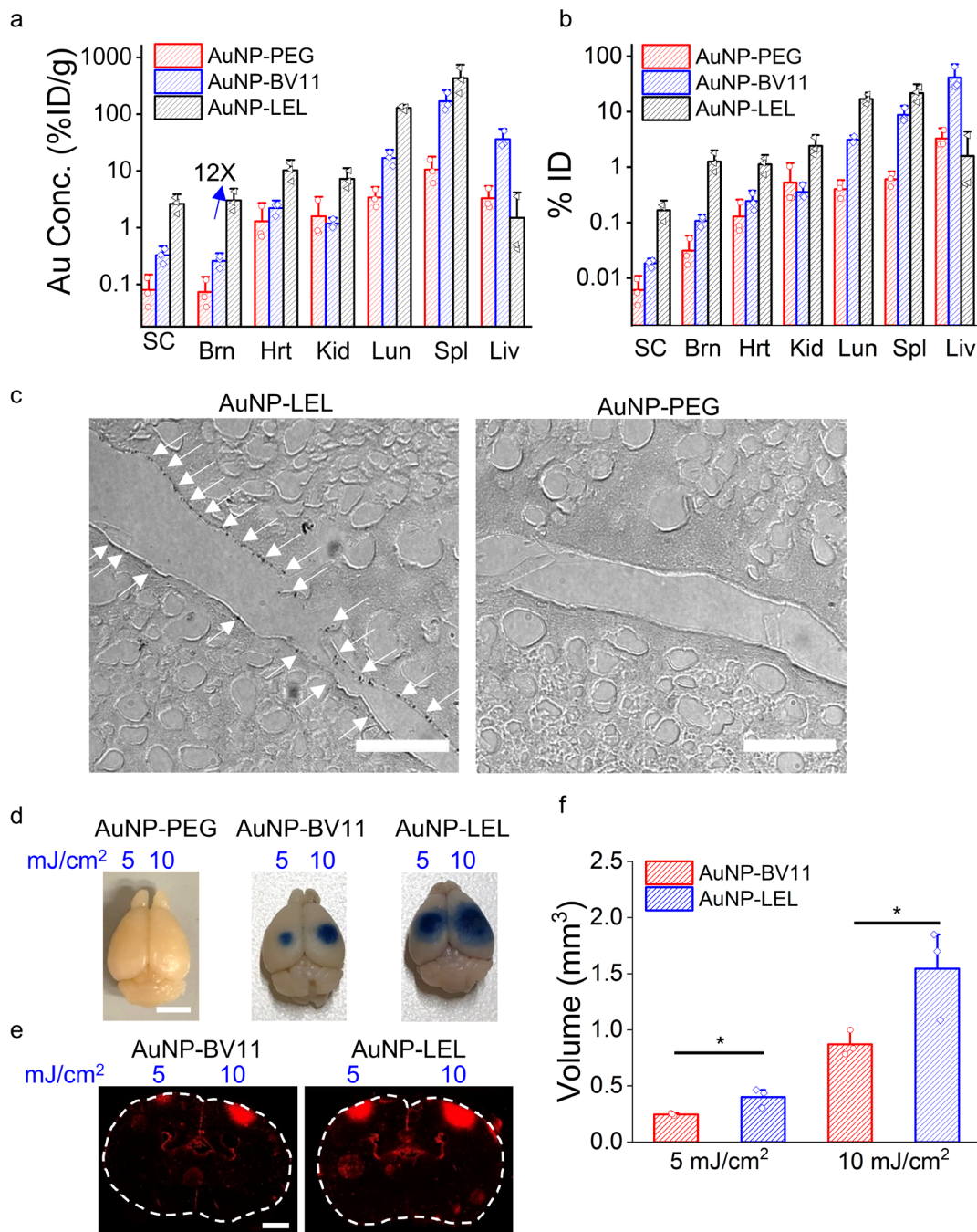


**Figure S9. BBB opening *in vivo* with different targets. (a-b)** The gold concentration in main organs with different targets expressed as % injection dose/gram organ weight (%ID/g) or % injection dose (%ID), respectively. Dose: 18.5  $\mu\text{g/g}$ . SC: spinal cord, Brn: brain, Hrt: heart, Kid: kidney, Lun: lung, Spl: spleen, Liv: liver. **(c)** AuNP-LEL are visualized by silver enhancement staining in the brain. The enhanced AuNPs are indicated by arrows. **(d)** Comparison of *in vivo* BBB opening by laser stimulation of AuNP-PEG, AuNP-BV11 and AuNP-LEL. Laser fluence was 5 and 10  $\text{mJ/cm}^2$ , 1 pulse. **(e)** Fluorescent images indicate Evans blue leakage. **(f)** Quantification of Evans blue leakage by total fluorescent volume. Data expressed as Mean  $\pm$  SD ( $n=3$  mice) in (a) and (e).

The statistical analysis in (f) was unpaired *t*-test, \* $p < 0.05$ . Scale bar: 20  $\mu\text{m}$  in (c), 4 mm in (d) and 1 mm in (e).

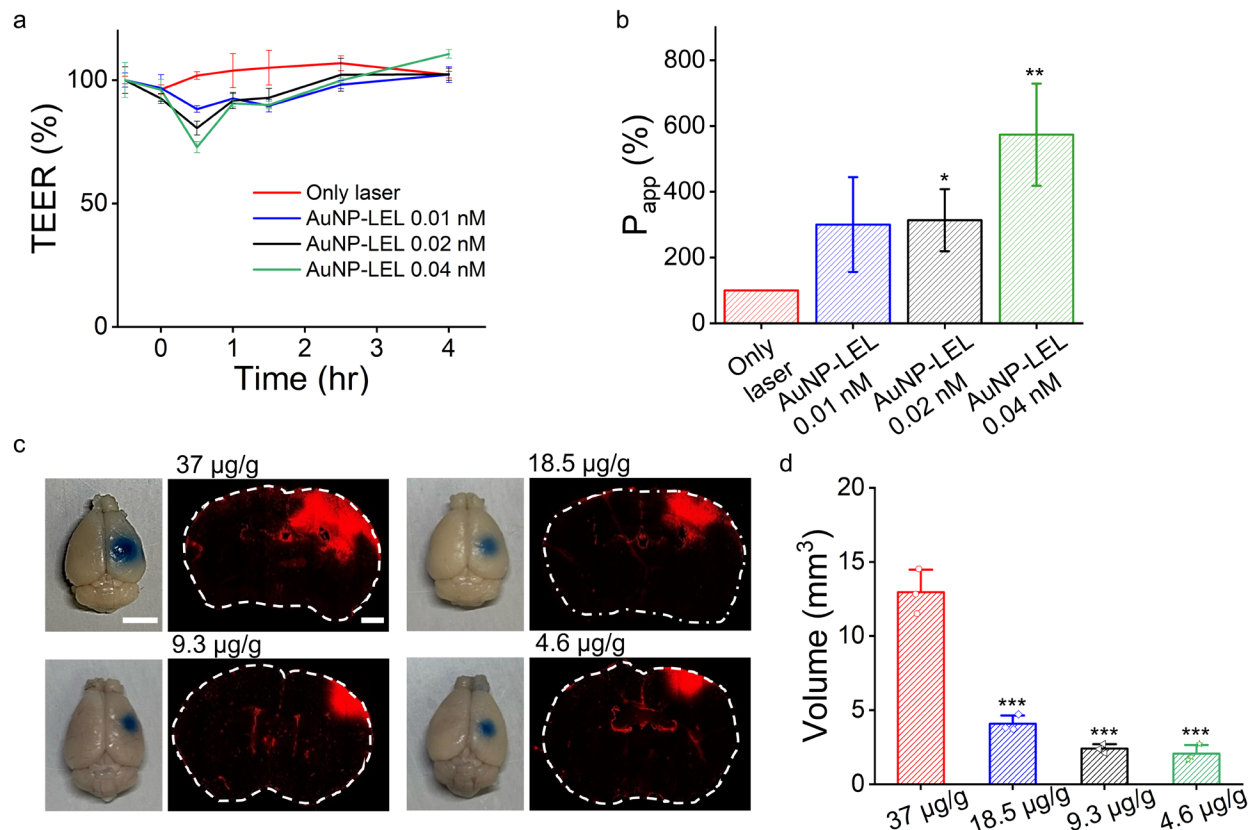


**Figure S10. Influence of AuNP-LEL dose-effect on optoBBB efficiency.** (a) Comparison of TEER change after laser irradiation of different doses of AuNP-LEL. Data is expressed as Mean  $\pm$  SD, n=3. (b) Comparison of permeability change after laser irradiation of different doses of AuNP-LEL. Data is expressed as Mean  $\pm$  SD n=3. (c) Comparison of Evans blue dye extravasation after laser irradiation of different doses of AuNP-LEL. (d) Quantification of Evans blue dye extravasation by total fluorescent volume. Data is expressed as Mean  $\pm$  SD (n=3 mice). Scale bar in c: 5 mm in the photographs and 1 mm in the fluorescent images. The laser parameter used was 35 mJ/cm<sup>2</sup>, 5 pulses, 5 Hz for (a-b), and 25 mJ/cm<sup>2</sup>, 1 pulse for (c).

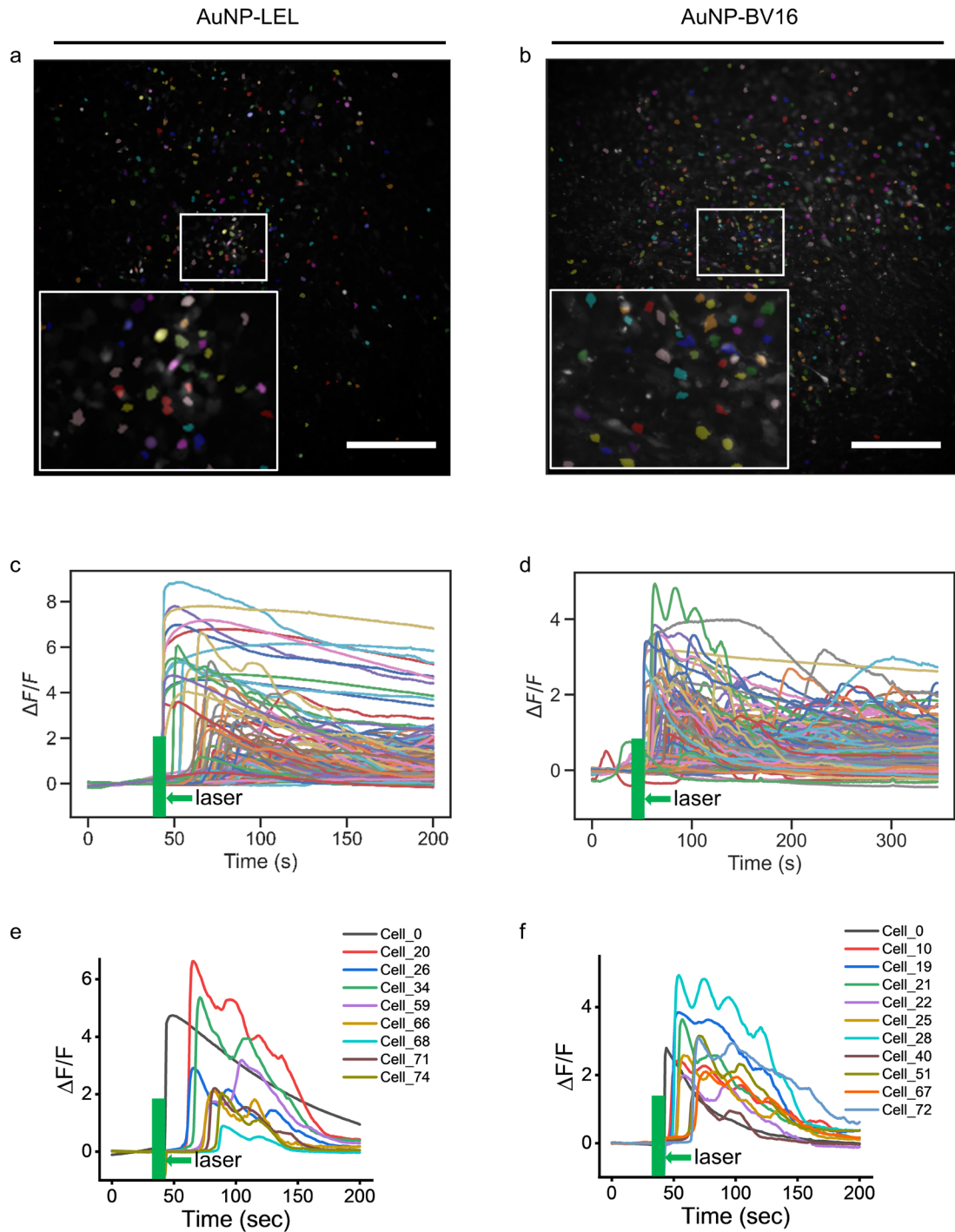


**Figure S11. Representative  $\text{Ca}^{2+}$  response from one experiment after laser stimulation of AuNP-LEL or AuNP-BV16. (a-b)** Segmentation of samples to show all the cells (labeled by different colors) that involve cytosolic  $\text{Ca}^{2+}$  elevation after laser stimulation. **(c-d)** The quantification of the  $\text{Ca}^{2+}$  signal of cells in (a) or (b). **(e-f)** Oscillatory increase in  $\text{Ca}^{2+}$  of cells in (a) or (b). 35mJ/cm<sup>2</sup>, 1 pulse. Scale bar: 0.5 mm.

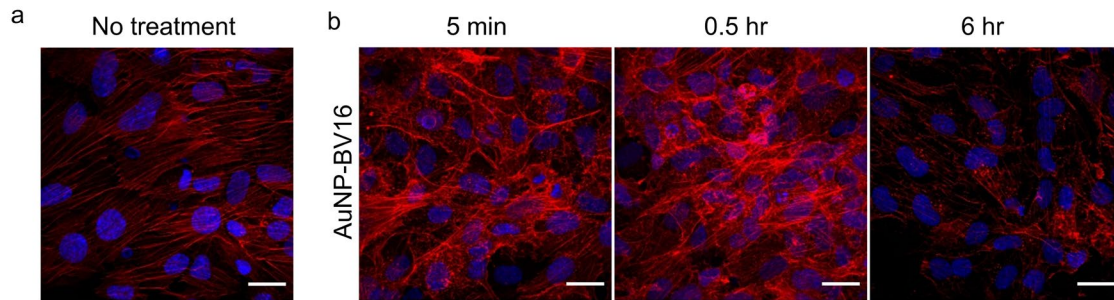


**Figure S12. Actin polymerization after laser stimulation of AuNP-BV16. (a)** F-actin staining of no treatment as control. **(b)** F-actin staining at 5 min, 0.5 hr, and 6 hr after laser stimulation of AuNP-BV16. 35 mJ/cm<sup>2</sup>, 1 pulse. Red: F-actin stained by phalloidin. Blue: nuclei. Scale bar: 20  $\mu$ m.